Published in *Smart Materials and Structures* 19(11), 11507 (2010)
(ISSN: 0964-1726, ESSN: 1361-665X)

Piezoelectric properties of lead-free Submicron-structured $(Bi_{0.5}Na_{0.5})_{0.94}Ba_{0.06}TiO_3$ ceramics from nanopowders

Lorena Pardo[1]*, Alvaro García[1], Klaus Brebøl[3], Elisa Mercadelli[2] and Carmen Galassi[2]

[1] *Instituto de Ciencia de Materiales de Madrid. Consejo Superior de Investigaciones Científicas (ICMM-CSIC). Cantoblanco. 28049- Madrid (Spain)*
[2] *Institute of Science and Technology for Ceramics- National Research Council (ISTEC - CNR) via Granarolo 64. I-48018 Faenza (Italy)*
[3]*Limiel ApS. Langebæk. (Denmark)*

**E-mail address :lpardo@icmm.csic.es*

keywords: ceramics, sol-gel synthesis, piezoelectricity, ferroelectricity
PACS:
piezoelectric materials, 77.84.-s
Dielectric materials, 77.84.-s; titanates, 77.84.Cg
Ferroelectric materials, 77.84.-s
Structure of crystalline solids, 61.66.-f
Materials treatment effects on microstructure, 81.40.-z

Abstract

Submicron-structured $(Bi_{0.5}Na_{0.5})_{0.94}Ba_{0.06}TiO_3$ (BNBT6) ceramics were obtained from nanometric powder synthesized by sol gel auto-combustion at 500ºC. Hot-pressing at low temperatures and a combination of this with re-crystallization, still moderate in order to reduce loss of the volatile elements, have been tested. Material properties, including all losses, were determined at the resonances of thin disks using Alemany et al. software. Ceramics hot pressed at 700-800ºC for 2h have a pseudo-cubic structure, grain size of few hundreds of nanometers and are homogeneous. Both their crystal structure and the lack of sintering prevent their poling. For ceramics hot-pressed at 950ºC for 3h, Bi or $(Bi_{0.5}Na_{0.5})$ loss, together with low piezoelectric properties (d_{33}=60 pC.N^{-1}, k_p=8%), was observed. Re-crystallization at 1000ºC-1h of ceramics hot-pressed at 700 and 800ºC for 2h keeps submicron-structure, reduces porosity and prevents off-stoichiometry. Mechanical and piezoelectric losses are also reduced and coupling factors increased (k_p=24.6%, k_t=36.4%). The best piezoelectric coefficient obtained in these ceramics (d_{33}=143 pC.N^{-1}) is comparable with those reported for coarse-grained ceramics.

Introduction

The search for lead-free compositions of high performance ferro-piezoelectric ceramics is a fast expanding research topic in the last few years, triggered by the environmental concern in Europe and the search for biocompatibility in medical applications [1-3].

The lead-free composition $Bi_{0.5}Na_{0.5}TiO_3$ (BNT) is known as ferroelectric shortly before 1961 [4]. BNT presents high conductivity, recently associated with loss of volatiles (Bi or ($Bi_{0.5}Na_{0.5}$)) at the sintering temperature [5], and coercive field that cause incomplete poling thus preventing its use as piezoceramic. For these reasons, a large number of solid-solution systems of increasing complexity [6-11] (BNT-$ATiO_3$(A=Ca, Sr, Ba and Pb), BNT-$Bi_{0.2}Sr_{0.7}TiO_3$, BNT–$KNbO_3$(KN), BNT-$Bi_{0.5}Li_{0.5}TiO_3$(BNLT), BNT-$Bi_{0.5}K_{0.5}TiO_3$(BNKT), BNT- $K_{0.5}Na_{0.5}NbO_3$(BNT-KNN), BNT-BKT-KNN, BNT-BT-KNN, BNT-BKT-$BiFeO_3$, BNT-BKT-$BaTiO_3$-$SrTiO_3$, etc.) have been tested and the improvement of their piezoelectric properties with respect to BNT demonstrated.

In particular, the (1-x) ($Bi_{0.5}Na_{0.5}$)TiO_3-x$BaTiO_3$ system of solid-solutions has been studied and it was found that there is a Morphotropic Phase Boundary (MPB), between rhombohedral and tetragonal ferroelectric phases at room temperature (RT), for compositions close to x=0.06 (BNBT6). Even if there are still a number of open questions about this composition, BNBT6 is considered a good candidate for lead-free piezoelectric ceramics due to the properties reported in the early 90´s [12,13]. Namely, an electromechanical coupling factor for thickness resonance of thin disks of k_t=52% and a d_{33} piezoelectric coefficient of 125pC.N^{-1} were measured for BNBT6 ceramics sintered for 1200ºC-2h in air.

Recently, several methods to obtain textured ceramics of the BNBT compositions at the MPB [14-17] were investigated. For (001) cuts, in fact, the single-crystals shows d_{33} values comparable, or even higher, than many PZT single-crystals [18]. The best reported

value for textured BNBT6 ceramic is d_{33}=241 $pC.N^{-1}$ for a microstructure consisting in highly oriented 10 μm x 3 μm platelets [16].

It is generally considered that the piezoelectric performance is improved when the grain size increases in the micron range, as a consequence of controlled enhancement in the sintering temperature to avoid a degraded final stage of sintering [19]. This was also observed for BNT-based ceramics [20-22]. However, few works have focussed on the investigation of the piezoelectric properties of nano- and submicron-structured lead-free piezoceramics [23,24]. The production of piezoceramics with suitable performance in this grain size range remains as a challenge.

BNBT6 ceramics have been recently obtained from powders synthesised by the sol gel auto-combustion method [25]. This synthesis method has been successfully used for the stoichiometry control and reduction of the processing temperature of piezoceramics, as well as to obtain primary particle size of few tens of nanometers.

It is well known that the final properties of ceramics are strongly related to the microstructures that dependent on the morphology of the starting powders. To obtain highly dense ceramics with controlled grain size, a combination of hot-pressing at reduced temperature and subsequent recrystallization at moderately higher temperature can be used [26].

The processing to obtain submicron-structured (1-x) $(Bi_{0.5}Na_{0.5})TiO_3$-x$BaTiO_3$ (with x=0.06) ceramics from nanometric powder synthesized by the sol gel auto-combustion method is presented in this work. Hot-pressing at low temperatures, as well as a combination of this and subsequent recrystallization at higher temperature, still moderate, in order to reduce Bi and Na loss, have been tested in the control of stoichiometry and ceramic microstructure. The piezoelectric, elastic and dielectric properties were determined at the

resonance of thin disks, thickness poled, and the potential use of the obtained ceramics is discussed.

Experimental method

(1-x) $(Bi_{0.5}Na_{0.5})TiO_3$-x$BaTiO_3$ with x=0.06 (BNBT6) nanometric (15-30 nm) powder was synthesized by a citrate nitrate sol gel auto-combustion method, details of which are explained elsewhere [25]. In this process, the pure perovskite phase is directly obtained by combusting the gel at 500ºC.

Green pellets of 15 mm diameter and 1 mm thickness were obtained by uniaxial and cold isostatic pressing the powder at 2000 $kg.cm^{-2}$. Hot-pressing was carried out using temperatures of 700, 800 and 950ºC, at 200 $kg.cm^{-2}$ in air, using heating and cooling rates of 3ºC.min^{-1}, and dwelling times of 1, 2 and 3h. In the light of the results on hot-pressed ceramics and to improve their piezoelectric properties, a combination of hot-pressing at low temperature, 700-800ºC for 2h, and subsequent recrystallization at higher temperature (1000ºC for 1h in air) has been used.

The density of the sintered samples was determined by Archimedes method. Ceramics were characterized using powder X-ray diffraction (XRD), with a Miniflex Rigaku (Japan) system operating with Ni filtered CuKa radiation, and a scanning electron microscopy (SEM) (Leica Cambridge Stereoscan 360) coupled with energy-dispersive X-ray spectrometry (EDS).

The P(E) hysteresis loops were recorded under sinusoidal waveform of amplitude of E_0=5 kV/mm and frequency f=1 Hz by using a modified Sawyer-Tower circuit.

Disks were grinded to a thickness to diameter ratio below 1/20 and Ag electrodes were attached at their major faces for poling and impedance measurements at the radial and thickness resonance modes. Poling was carried out at 180ºC in a silicone oil bath up to fields

of 40-60 kV.cm^{-1}, depending on the slightly variable dielectric strength of the samples. d_{33} piezoelectric coefficients were measured in a Berlincourt meter a day after samples poling.

Complex impedance measurements at resonance were carried on using a HP4192A impedance analyzer controlled by a computer via a GPIB-PCIIA (National Instruments) interface board. Alemany et al. software was used here, to avoid the drawbacks of the Standard methods [27], for the calculation of the piezoelectric, elastic and dielectric coefficients, including all losses, in each mode of resonance, as well as for the determination of the corresponding electromechanical coupling factors and frequency numbers. Details of the calculations are explained elsewhere for the thickness [28] and planar resonances [29] of thin disks, poled and excited in thickness. In this software the material coefficients in complex form (P*=P′- iP′′) are determined by solving a set of non-linear equations that results when experimental impedance data at a number of frequencies are introduced into the appropriate analytical solution of the wave equation for a given resonance mode. After measurement of the complex impedance (Z*) or its inverse, the admittance (Y*), depending on the resonance mode, plots of the peaks of the a.c. resistance (R) and conductance (G), real parts of the impedance (Z*=R+iX) and admittance (Y*= G+iB), respectively, are traced as a function of the frequency. The maxima of these two peaks determine two of the characteristic frequencies of the resonance, f_p and f_s, respectively, that are needed for the calculation. The rest of the frequencies are automatically determined by the software. After the calculation of the complex parameters, the resonance spectrum is reconstructed as an accuracy test of the final set of calculated coefficients. This accuracy is also quantitatively characterized by the regression factor (R^2) of such reconstruction to the experimental spectrum. It has to be mentioned that there is a good agreement between the real part of the coefficients calculated by this method [28] and the standard ones [27]. This method also provides the imaginary part of the complex parameters thus giving the additional information of all the material losses.

Experimental results

All BNBT6 ceramics showed similar XRD patterns corresponding to the pure perovskite phase (Figure 1) and secondary phases were not observed. Moreover all these patterns show peak broadening. For the structure found at the rhombohedral-tetragonal MPB of this solid solution [30, 31], the X-ray diffraction pattern is characterized by the splitting of the peak (111) at about 2θ=40°, that corresponds to the tetragonal symmetry ($BaTiO_3$-like), into two separated peaks, corresponding to the (006) and (202) planes in hexagonal description [32] (JCPDS file #70-9850), related to the rhombohedral one (BNT-like). This takes place together with the splitting of the (024) peak of the rhombohedral symmetry, at around 2θ =46.5°, into (002) and (200) planes, characteristic of the tetragonal one. Figures 2(a) and (b) show slow scans made from 39 to 41 º2θ and from 45 to 48 º2θ, respectively, for all ceramics, after crushing the samples to avoid surface effects.

Ceramics hot pressed at 700ºC-2h and 800ºC-2h presented a white colour and poor mechanical stability due to incomplete sintering at these low temperatures. The maximum relative density achieved for these is 84% (theoretical density for the nominal composition is 5.9245 $g.cm^{-3}$). Only the ceramics hot-pressed at 950ºC show a porosity free bright aspect, a glassy fracture (for the sample hot-pressed at 950ºC-3h) and relative density up to 99%. Recrystallised ceramics after hot-pressing are highly dense with typical brittle fracture. Maximum relative density achieved is 96%.

Figure 3 shows the energy dispersive X-ray spectra (EDS), and backscattered electrons (BSE) SEM micrographs of the same area, for ceramics hot-pressed at 700ºC-2h (Figure 3(a)), 800ºC-2h (Figure 3(b)) and 950ºC-3h (Figure 3(c)). The surfaces seem to be compositionally homogeneous for 700ºC-2h (identical spectrum obtained in two randomly chosen locations of the surface) and 800ºC-2h. Corresponding SEM micrographs shows that these hot-pressed ceramics have a very fine grain structure. Average grain size is in the range

of hundreds of nanometers. For the ceramics hot pressed at 950ºC-3h the BSE SEM micrograph reveals a noticeable amount of brighter grains than the overall matrix at the studied surface. These are slightly Bi rich as revealed by the comparative EDS results in two points of this surface (Figure 3(c)).

Figures 4, 5 and 6 show the SEM images of the fractures and of the polished and thermally etched surfaces of the samples hot-pressed at 950ºC and the recrystallised ones, respectively. All hot-pressed ceramics, even those prepared at the highest temperature and longer time, 950ºC 3h (Figure 4(f)), present average grain size below 1μm. The ceramic hot-pressed at 950ºC-1h has very fine grains (~200 nm) surrounding the bigger grains (Figure 4(b)). As the hot-pressing time increases and the sintering proceeds, these ultra-fine grains progressively disappear (Figure 4(d)) to give place to a homogeneous microstructure at 950ºC-3h (Figure 4(f)). Ceramics hot-pressed at 950ºC present transgranular fracture, with a small amount of residual porosity. As expected, porosity decreases as the hot-pressing time increases and all these hot-pressed ceramics have a homogeneously distributed intergranular porosity.

The ceramic recrystallised at 1000ºC-1h after hot-pressing at 700ºC-2h presents intergranular fracture (Figure 5(a)). The grain size is also below 1μm, with a population of grains below 500nm, and the porosity is intergranular (Figure 5(b)). The amount of porosity is much higher than in the ceramic hot pressed at 950ºC-3h (Figure 4(e)).

The ceramic recrystallised at 1000ºC-1h after hot-pressing at 800ºC-2h shows transgranular fracture (Figure 6(a)) and slightly higher grain size, close to 1μm (Figure 6(b)), together with less residual porosity than the previous sample.

The backscattered electron SEM micrographs (Figure 5(c) and 6(c)) of the ceramics recrystallised at 1000ºC-1h after hot-pressing, and the corresponding EDS spectra not shown

here, indicate that the loss of volatiles is not as extended in the surface as it was observed for the ceramic hot-pressed at 950ºC-3h (Figure 3(c)).

Both their pseudo-cubic structure (see Figures 2(a) and (b)) and the lack of efficient sintering prevent the polarization of ceramics hot-pressed at 700 and 800ºC-2h. Only the ceramics hot-pressed at 950ºC and the recrystallised ones could be poled and their piezoelectric properties could be obtained. Table 1 summarizes the range of grain size, relative density and the piezoelectric (d_{31}), elastic (s_{11}^E, s_{12}^E) and dielectric (ε^T_{33}) linear coefficients, as well as the electromechanical coupling factors (k_p, k_t) and frequency numbers (N_p, N_t), measured at the planar and thickness resonances of thin disks. Measured values are compared in Table 1 with published data for air-sintered ceramics obtained from sol-gel [25] and mixed oxides [12,31,33] and for textured ceramics obtained by templated grain growth [14].

Figure 7 shows subcoercive ferroelectric hysteresis loop at room temperature of the ceramic hot-pressed at 950ºC-3h, with the lowest porosity (Figure 4(e)) among the studied ceramics, compared with a coarser grained ceramic prepared from mixed oxides method and sintered in air at 1100ºC-2h [33].

Figure 8 presents the experimental spectra (symbols), R and G vs. frequency peaks, for the radial and thickness resonance modes of thin disks of ceramics recrystallised at 1000ºC-1h after hot pressing (at 700ºC and 800ºC for 2h). The reconstructed spectra (lines) after calculation of the material parameters by Alemany et al. software are also shown.

Discussion

Neither the splitting of the peaks (006) and (202) at 2θ ~40º (Figure 2(a)), that will show the presence of the rhombohedral feature of the structure, nor the splitting of the (002) and (200) peaks at 2θ ~46.5º (Figure 2(b)), of the tetragonal one, can be clearly observed in

any of the ceramics, most probably due to peak broadening. On the other hand, some authors have already suggested that the MPB could have a pseudo-cubic or tetragonal structure [34], which could be the case of the ceramics hot pressed at 700 and 800ºC that present symmetric peaks. The grain size of the ceramics increases, and the widening of the peaks is expected to reduce, as the hot-pressing temperature increases (Figure 3) and, also, after recrystallization (Figures 5 and 6). However, wide and symmetric peak profiles at both intervals of º2θ are also observed for ceramics hot-pressed at 950ºC for 1 and 2 h. The sample hot-pressed at 950ºC for 3h and those recrystallised at 1000ºC for 1h show displacement of the peaks to lower angles, and even if the peaks at Figure 2(a) are still symmetric (but still wide), those of Figure 2(b) are asymmetric. This could be related to some incipient peak splitting that could indicate a tendency to the tetragonal-like symmetry in the sample hot-pressed at 950ºC for 3h and the recrystallised ceramics. The main feature observed for all ceramics is the widening and absence of clear peak splitting, which can be attributed to a nano- or submicron-grain size observed at the SEM images.

It has been previously pointed out that BNBT ceramics at the MPB possess relatively large ratio of k_t/k_p, low dielectric constant and high frequency constant. The d_{33} ~100 $pC.N^{-1}$ and loss tangent ~0.02 are also characteristic of these ceramics.

The piezoelectric properties measured for the ceramics hot pressed at 950ºC are not in agreement with those reported for coarse grained ceramics in the literature, as summarised by the overall description given above. Their piezoelectric properties are lower even for the sample prepared at 950ºC-3h that is almost fully dense (Figure 4(e)) and presents a homogeneous microstructure (Figure 4(f)).

On the one hand, ceramics hot pressed at 950ºC can be poled due to proper sintering. The study of the effect of A-site non-stoichiometry in similar ceramics (BNBT8) showed that both reduction and increase of $(Na_{0.5}Bi_{0.5})$ result in an increase of the piezoelectric properties

[31] because both, respectively, produce A or B-vacancies in the perovskite structure that could relax the strain caused by non-180º domain orientation. Despite of the fact that they are submicron structured, like the hot pressed ceramics at 700ºC and 800ºC, proper sintering and some degree of off-stoichiometry gives place to measurable piezoelectric properties in the ceramics hot-pressed at 950ºC. On the other hand, at increasing hot-pressing time, a significant loss of the most volatile elements, Bi or ($Na_{0.5}Bi_{0.5}$), can take place. This loss could shift the composition to the Ba richer side of BNBT solid solution (tetragonal, $BaTiO_3$-like) near the MPB. This is consistent with XRD (Figure 2) and EDS results shown in Figure 3(c) for hot-pressing at 950ºC-3h. These ceramics are off-stoichiometric and most probably present some zones of tetragonal ferroelectric phase, which leads to lower (d_{33}=53-60 $pC.N^{-1}$, k_t= 9.5%) piezoelectric properties than the MPB composition [31]. Besides, non-180º domain reorientation generates some strain. As the ceramic hot-pressed at 950ºC-3h shows virtually zero residual porosity (Figure 4(e)), intergranular stress can originate from that strain that switches back the oriented non-180º domains to their original orientation when the poling field is removed thus reducing the remanent polarization. The comparison of the ferroelectric hysteresis loop of this ceramic (Figure 7) with a coarser grained ceramic prepared from mixed oxides method confirms this assumption. While the field for polarization reversal is similar for both ceramics, the hot-pressed one cannot be poled to saturation under the same field and presents lower remanent polarization and, consequently, lower piezoelectric activity (see Table 1).

Whereas ($Na_{0.5}Bi_{0.5}$) loss results in an increase of permittivity and losses, the addition of ($Na_{0.5}Bi_{0.5}$) causes its decrease [5]. Besides, it has also been observed that, approaching grain sizes of ~1μm in BNT ceramics [21], the permittivity increases as the grain size decreases. This could explain the high permittivity values obtained for the ceramics hot-pressed at 950ºC for 1 and 2h, accompanied by high dielectric losses.

It is noticeable that the ceramics hot-pressed at 950ºC show a lower ratio k_t/k_p~ 1.1 than the first reported for coarser grained air sintered ceramics k_t/k_p= 2.6 [10]. Similar decrease of k_t/k_p ratio was found [16] for highly textured BNBT6 ceramic with k_t/k_p =1.6 (k_p= 41.2%, k_t=66.5%). Other values of k_t/k_p =1.4 [31], 1.6 [25] and 1,9 [33] have been reported for coarser grained ceramics.

Figure 8 shows the resonance spectra of planar and thickness modes of the ceramics recrystallised at 1000ºC-1h after hot-pressing. For both ceramics the regression factors of the recalculated to the experimental curves are high and allow the accurate calculation of both real parts of the coefficients and corresponding losses, including the piezoelectric ones, shown in Table 1.

The piezoelectric characterization for the ceramic hot-pressed at 700ºC-2h and recrystallised at 1000ºC-1h (Table 1) shows a clear improvement over the results on the hot-pressed ceramic at 950ºC-3h. Taking into account that the grain size of the recrystallised ceramic after hot-pressing at 700ºC-2h is not significantly higher (Figure 5(b)) than the hot-pressed ceramics at 950ºC-3h one (Figure 4(f)), the better properties of the recrystallised ceramic are most probably due to the better stoichiometry (Figure 5(c)) and the easier non-180º domain reorientation caused by the presence of homogeneously distributed porosity (Figure 5(a)). Therefore, the recrystallised ceramic can be better poled and its piezoelectric activity is improved (d_{33}=105 $pC.N^{-1}$, k_t=29.5%). However, the population of small grains in the inhomogeneous microstructure reflect in the high losses (elastic and dielectric) that are a drawback for practical applications.

For the ceramic recrystallised at 1000ºC-1h after hot-pressing at 800ºC-2h a moderate loss of volatiles is observed (Figure 6(c)). This loss, combined with the hot pressing and recrystallization conditions, seems to promote inhomogeneous microstructures as it was already observed for a similar composition [33]. The samples present needle-like structures

that differ from the matrix characterized by elongated grains (Figure 6(b)). The EDS analysis, not shown here, reveals that, in comparison with the matrix phase, the composition of the needle-like structure is Ba rich (Figure 6(c)). The best properties were obtained for this ceramic (Table 1 and Figure 8). As above mentioned for the hot-pressed ceramics at 700ºC-2h and recrystallised at 1000ºC-1h, an increasing polarizability with respect to the previously discussed ceramics could lead to better piezoelectric properties. This ceramic shows high a d_{33} (143 $pC.N^{-1}$) that is comparable or higher than those reported for non-textured ceramics of undoped BNBT6 composition, despite of their larger grain size resulting from the higher processing temperature (1100-1200ºC) [12, 25, 31, 33, 35]. This is accompanied by high frequency numbers, lower piezoelectric and mechanical losses and high dielectric permittivity, most probably due to a lower residual porosity.

The good piezoelectric performance of the submicron-structured ceramics here obtained at relatively low temperatures is, most probably, the result of the related good stoichiometry and low conductivity that allows poling at 180ºC. The literature reports results of low temperature poling (RT [5], 60ºC [12], 80ºC [31,34], 100ºC [14]), poling for long times at 120ºC [25,33] or even non-specified conditions. Poling conditions are limited by the conductivity of the samples, which is mainly due to the loss of volatiles, in BNT or BNBT6 ceramics. However, above ~100ºC, which is the temperature reported [6,31] for a dielectric anomaly in BNBT6, a coexistence of phases is expected, similarly to what it is observed in BNT [32, 36]. These are the RT ferroelectric (rhombohedral) phase and a non-polar at zero field (tetragonal) phase. This coexistence extends up to the temperature of the maximum dielectric permittivity (~300ºC for BNBT6). As it happens in the MPB composition, the coexistence of phases with different crystal symmetry increases the number of allowed crystal directions for alignment of the polarization with the poling field, thus giving place to higher remanent polarization and enhanced piezoelectric coefficients.

For a material to be considered of interest as ultrasonic transducer for medical applications it should have a combination of high electromechanical coupling coefficient for the relevant vibration mode (thickness mode) and low acoustic impedance, $Z = \rho .c$ (where c=speed of sound in the material=$2N_t$ and ρ is the material density), for matching with the propagation media. The ceramic hot-pressed at 800ºC-2h and recrystallised at 1000ºC-1h shows a combination of Z=25MRayls and k_t=36.4%. Besides, for high frequency devices or for arrays, whenever small dimensions of the ceramic element must be achieved, fine-grained materials are required. All these characteristics make this recrystallised ceramic a good candidate as lead-free piezoceramic.

Conclusions

Submicron-structured, single-phase, lead-free piezoelectric ceramics of (1-x) $(Bi_{0.5}Na_{0.5})TiO_3$-$xBaTiO_3$, with x=0.06 (BNBT6), were obtained by hot-pressing from nanometric powder synthesized by the sol gel auto-combustion method.

Ceramics hot-pressed at 700ºC and 800ºC for 2h showed homogeneous microstructures of grain size below 500nm and a pseudo-cubic structure. Both their crystal structure and the lack of sintering prevent the poling of these ceramics.

Ceramics hot-pressed at 950ºC have grain sizes well below 1μm. The one hot-pressed at 950ºC-3h shows plausible coexistence of tetragonal and MPB symmetry of the ferroelectric perovskite-type structure. This is consistent with the evidence of Bi or $(Na_{0.5}Bi_{0.5})$ loss at the surface found by EDS analysis. The ceramic hot-pressed at 950ºC-3h showed maximum values of d_{33}=60 $pC.N^{-1}$, k_p=8% and low k_t/k_p~ 1. Both the tetragonal phase and the intergranular stresses, due to the virtually zero residual porosity, prevent to obtain higher piezoelectric coefficients in this ceramic.

It has been proved here the principle of enhancing the piezoelectric performance of BNBT6 ceramics hot-pressed at low temperature (700ºC-800ºC for 2h) by recrystallization at a moderately higher temperature (1000ºC for 1h). Low processing temperatures prevent extensive off-stoichiometry and keep submicron structures, while this treatment reduces the porosity at the same time. All this results in the reduced ceramic conductivity, which makes possible the poling at 180ºC that, most probably due to the coexistence of phases at such temperature, built up high remanent polarization. The best piezoelectric coefficient obtained for the fine-grained ceramics (d_{33}=143pC.N^{-1}, k_p=24.6%, k_t=36.4%) are comparable with those reported for coarse-grained BNBT6 ceramics sintered in air at higher temperatures (1100-1200ºC) and higher than recently published results for more complex compositions.

Acknowledgments
ELENA COST539 Action (ESF) and European Network of Excellence on Multifunctional & Integrated piezoelectric Devices (NoE-MIND CE FP6 515757-2).

References
[1] Y. Saito, H. Takao, T. Tani, T. Nonoyama, K. Takatori, T. Homma, T. Nagaya and M. Nakamura (2004) *Nature,* 432 84-87.
[2] E. Ringgaard and T. Wurlitzer (2005) *J. Eur. Ceram. Soc.*, 25 (12) 2701-2706.
[3] J. Rodel, W. Jo, K.T.P. Seifert, E.M. Anton,T. Granzow and D. Damjanovic (2009) *J.Am. Ceram. Soc*., 92 1153-1177.
[4] G.A.Smolenskii, V.A. Isupov, A.I. Agranovskaya and N.N. Krainik (1961) *Soviet Physics Solid State*, 2 (11) 2651-2654.
[5] Y. Hiruma, H. Nagata and T. Takenaka (2009) *J. Appl. Phys*., 105 084112- 084112-8.
[6] T.Takenaka, H. Nagata and Y. Hiruma (2009) *IEEE Trans. Ultrasonics, Ferroelectrics and Frequency Control*, 56(8) 1595-1612.
[7] C. Ang and Z. Yu. (2009) *Appl. Phys. Lett.*, 95 2329081-2329083.
[8] S.T. Zhang, A.B. Kounga, W. Jo, C. Jamin, K. Seifert, T. Granzow, J. Rodel and D. Damjanovic (2009) *Adv. Mater.*, 21 4716–4720.
[9] S.T. Zhang, L.Wang, Y. F. Chen and A.B. Kounga (2010) *J. Am. Ceram. Soc*., Rapid Comm., in press DOI: 10.1111/j.1551-2916.2009.03592.x
[10] C. Zhou, X. Liu,W. Li, C. Yuan (2009) *Mat.Chem.Phys.* 114 832–836.
[11] D. Lin and K.W. Kwok (2010) *J. Am. Ceram. Soc.*, 93 (3) 806-813.
[12] T. Takenaka, K.Maruyama and K. Sakata (1991*) Jap. J. Appl. Phys*., 30(9B) 2236-2239.
[13] T. Takenaka, A. Huzumi, T. Hata and K. Sakata (1993) *Silicates Industrials*, 7(8) 136-142.
[14] H. Yilmaz, S. Trolier-Mckinstry and G.L. Messing (2003) *J. Electroceram.,* 11 217-226.
[15] D.S. Lee, S.J. Jeong, E.C. Park, J. S. Song (2006) *J. Electroceram.,* 17 505–508.
[16] Y. K. Yan, H. P. Zhou, W. Zhao and D. Liu (2008) *J. Electroceram.,* 21 246–250

[17] M. Wu, Y. Li, D. Wang, J. Zeng and Q. Yin (2009) *J. Electroceram.*, 22 131–135
[18] Y.M.Chiang, G.W. Farrey and A.N. Soukhojak (1998) *Appl. Phys.Lett.*, 73(25) 3683-3685.
[19] J. Ricote J, C. Alemany and L. Pardo (1995) *J. Mater. Res*., 10(12) 3194-3203.
[20] A. Herabut and A. Safari (1997) *J. Am. Ceram. Soc.*, 80(11) 2954–58.
[21] L. Liu and H. Fan (2006) *J. Electroceram.*, 16 293-296.
[22] O. Khamman A. Watcharapasorn K. Pengpat and T. Tunkasiri (2006) *J. Mater. Sci.*, 41 5391–5394.
[23] A. Moure, T.Hungría, A.Castro and L. Pardo(2009) *J. Eur. Ceram. Soc.*, 29 2297-2308.
[24] A. Moure, T.Hungría, A.Castro and L. Pardo(2010) *J. Mater. Sci.*, 45 1211–1219
[25] E. Mercadelli E, C. Galassi, A.L. Costa, S.Albonetti and A. Sansón (2008) *J. Sol-Gel Sci. Tech.*, 46(1) 39-45.
[26] A. Moure, A. Castro and L. Pardo(2004) *Acta Mater.*, 52 945-957.
[27] "IEEE Standard on piezoelectricity". ANSI/IEEE Std. 176-1987. "Piezoelectric properties of ceramic materials and components. Part 2: methods of measurement – Low power". European Standard CENELEC, EN 50324-2 (2002).
[28] C. Alemany, L. Pardo, B. Jiménez, F. Carmona, J. Mendiola and A.M. González (1994) *J. Phys. D: Appl. Phys.*, 27 148-155.
[29] C. Alemany, A. M. Gónzalez, L. Pardo, B. Jiménez, F. Carmona, J. Mendiola (1995) *J. Phys. D: Appl. Phys.*, 28 945-956.
[30] X.X. Wang, H.L.W. Chan, C.L. Choy (2005) *Appl. Phys. A*, 80 333-336.
[31] B.J. Chu, D.R. Chen, G.R. Li and Q.R. Yin (2002) *J. Eur.Ceram. Soc*., 22 2115–2121.
[32] G.O Jones and P.A.Thomas (2002) *Acta Crystallographica B*, 58 168-178.
[33] E. Mercadelli, A. Sanson, C. Capiani, A. L. Costa, C. Galassi (2009) *Processing and Application of Ceramics*, 3(1-2) 73-78.
[34] R. Ranjan and A. Dviwedi (2005) *Sol. State Com.*, 135 394-399.
[35] Q. Xu, S. Chen, W. Chen, S. Wu, J. Zhou, H. Sun and Y. Li (2005) *Mat. Chem. Phys.*, 90 111-115.
[36] C.S. Tu, S.H. Huang, C.S. Ku, H.Y. Lee, R.R. Chien, V.H. Schmidt and H. Luo (2010) *Appl. Phys. Lett.*, 96 062903-062906.

Table Caption

Table I. Processing conditions, relative density, range of grain size, and piezoelectric, elastic and dielectric parameters, as well as electromechanical coupling factors and frequency numbers, obtained from planar and thickness resonances of the thin ceramics disk, poled and excited in thickness, in comparison with data in the literature. (*d_{33} from Berlincourt-meter; ** ε^{T}_{33} and tan δ measured at 1 kHz)

Table I.

Composition and synthesis route	BNBT6 from sol-gel autocombustion nanopowder								BNBT6 mixed oxides	BNBT6 mixed oxides	BNBT6 mixed oxides	BNBT6
Processing conditions	HP 700ºC 2h	HP 800ºC 2h	HP 950ºC 1h	HP 950ºC 2h	HP 950ºC 3h	HP 700ºC 2h + recrystallised 1000ºC-1h	HP 800ºC 2h + recrystallised 1000°C-1h	sintering 1100ºC 2h (ref. 25)	sintering 1200ºC 2h (ref. 12)	sintering 1150°C 2h (ref. 33)	sintering 1160-1180ºC 1h (ref. 31)	TGG 1200ºC 48h (ref. 14)
Relative density (%)	77	84	91	91	99	83	96	97	98	96	---	93
Grain size range	<500 nm	<500 nm	<1μm	<1μm	~1μm	<1μm	~1μm	≥1μm	>3μm	>3μm	>3μm	15μm
d_{33} ($pC.N^{-1}$)*	---	---	45	36	53-60	105	143	125	125	131	122	200
d_{31} ($pC.N^{-1}$)	--	--	-13.39	-14.12	- 9.2+0.2 i	-19.9+0.97i	-34.8+1.37	-38.61	40	-36.8	---	---
k_p(%)	---	---	5.9	5.6	8.3	13.6	24.6	27.2	20	26.5	29	30.1
k_t(%)	---	---	6.6	6.4	9.5	29.5	36.4	42.6	52	50.4	40	---
N_p(kHz.mm)	---	---	2521	2459	3204	2535	2873	2953	3000	2937	3000	---
N_t(kHz.mm)	---	---	2197	2268	2219	1855	2238	2409	2600	2293	2522	---
ε^T_{33}	---	---	1206	1323	434 - 21 i	465 - 24 i	636 – 34i	698	580**	648	601**	716**
tan δ	---	---	0.278	0.381	0.048	0.052	0.054	0.030	0.013	0.023	0.018	0.039
σ			0.20	0.19	0.29	0.27	0.27	0.29	---	0.26	0.25	---
s^E_{11} (10^{-12} m^2N^{-1})	--	--	12.1	13.7	8.95 - 0.18i	14.30 - 0.20 i	9.57-0.09i	9.23	8.59	9.01	---	---
s^E_{12} (10^{-12} m^2N^{-1})	--	--	-2.40	-2.65	-2.60+ 0.05i	-3.9 + 0.05i	-2.90+0.03i	-2.69	---	-2.31	---	---

Figure Captions

Figure 1. XRD patterns indexed for the pseudo-cubic symmetry of sintered BNBT samples: a) hot pressed (HP) at 700ºC-2h, b) HP at 800ºC-2h, c) HP at 950ºC-1h, d) HP at 950ºC-2h, e) HP at 950ºC-3h, f) HP at 700ºC-2h and re-crystallized at 1000ºC-1h, g) HP at 800ºC-2h and re-crystallized at 1000ºC-1h.

Figure 2. Detail of the XRD pattern at the 2 interval: (a) of the (006) and (202) peaks and (b) of the (002) and (200) peaks for the same ceramics as in Figure 1.

Figure 3. Energy dispersive X-ray spectra (EDS), and backscattered electrons SEM micrographs of the area in which these were obtained (marked with labels) for hot-pressed ceramics at (a) 700ºC-2h, (b) 800ºC-2h and (c) 950ºC-3h.

Figure 4. Scanning electron micrographs of fracture and polished and thermally etched surface, respectively, of (a) and (b) ceramic hot pressed at 950°C-1h, (c) and (d) ceramic hot pressed at 950°C-2h and (e) and (f) ceramic hot pressed at 950°C-3h.

Figure 5. Scanning electron micrographs (SEM) of (a) fracture and (b) polished and thermally etched surface, respectively, and (c) backscattered electrons SEM image of the ceramic hot pressed at 700°C-2h and re-crystallized at 1000ºC-1h.

Figure 6. Scanning electron micrographs (SEM) of (a) fracture and (b) polished and thermally etched surface, respectively, and (c) backscattered electrons SEM image of the ceramic hot pressed at 800°C-2h and re-crystallized at 1000ºC-1h.

Figure 7. Ferroelectric hysteresis loop of the ceramic hot-pressed at 950ºC-3h, in comparison with the ceramic prepared from mixed oxides and sintered in air at 1100ºC-2h (reference 31).

Figure 8. Spectra of planar and thickness resonance for thin disks of ceramics recrystallised at 1000ºC-1h after hot pressing at 700ºC-2h (upper line; R^2(planar)=0.9976 and R^2(thickness)=0.9909) and 800ºC- 2h (lower line; R^2(planar)=0.9997 and R^2(thickness)=0.9735). The experimental data (symbols) and the reconstructed spectra (lines) after calculation of the material parameters by Alemany et al. software are shown.

Figure 1.

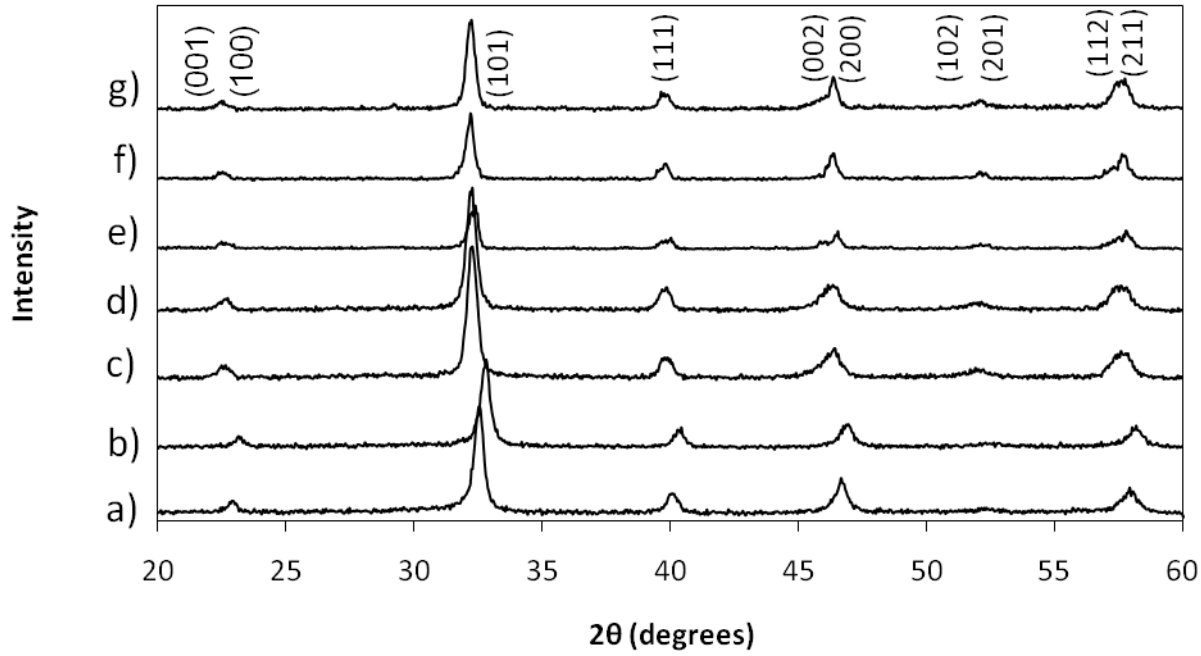

"Piezoelectric properties of lead-free Submicron-structured …"
L. Pardo et al.

Figure 2.

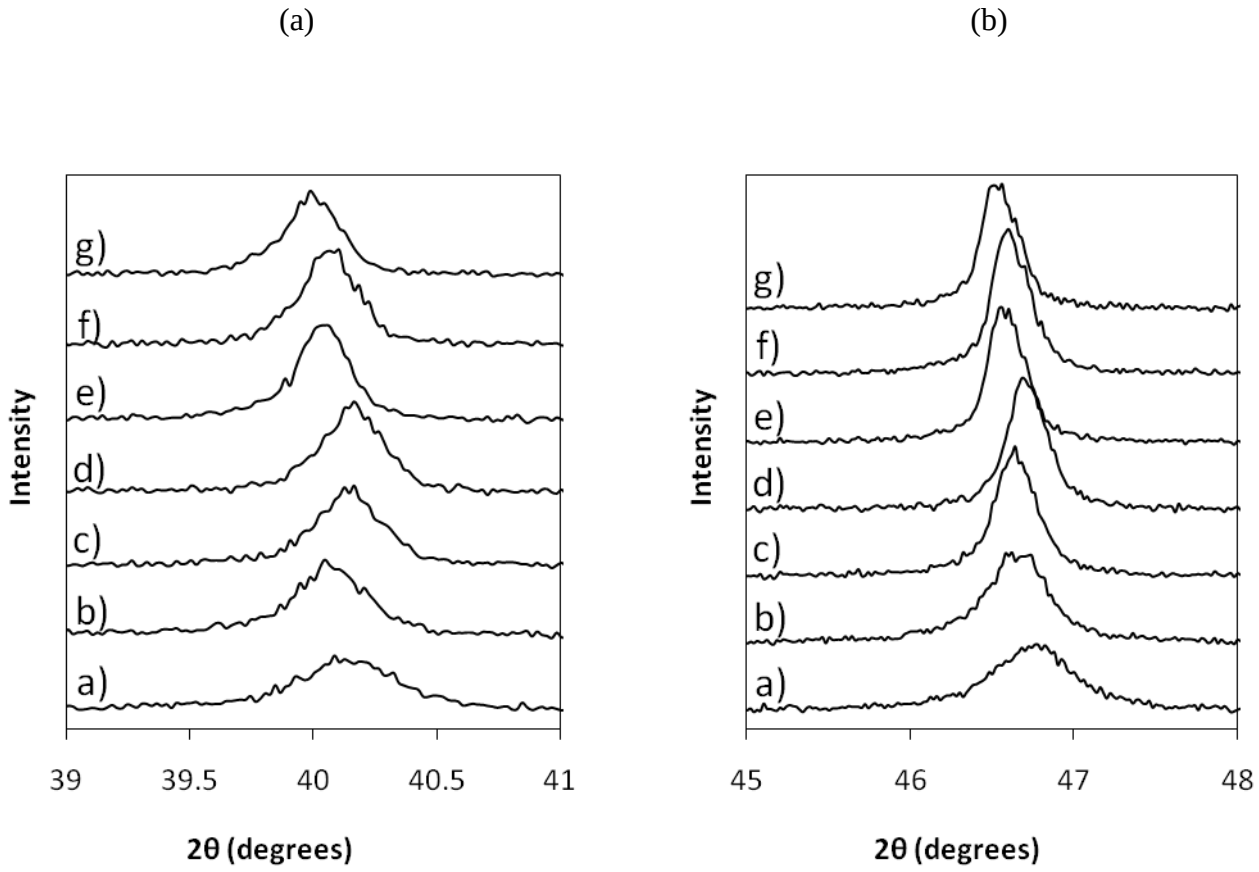

"Piezoelectric properties of lead-free Submicron-structured …"
L. Pardo et al.

Figure 3(a). “Piezoelectric properties of lead-free Submicron-structured …”
L. Pardo et al.

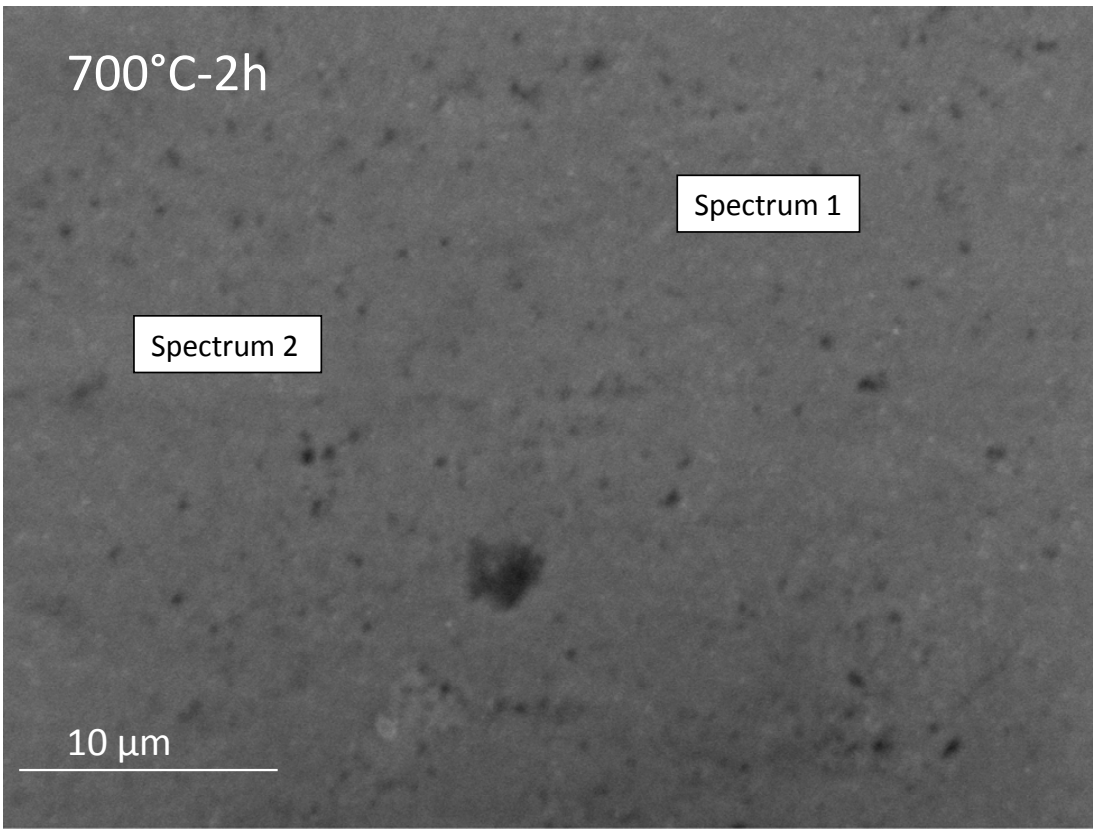

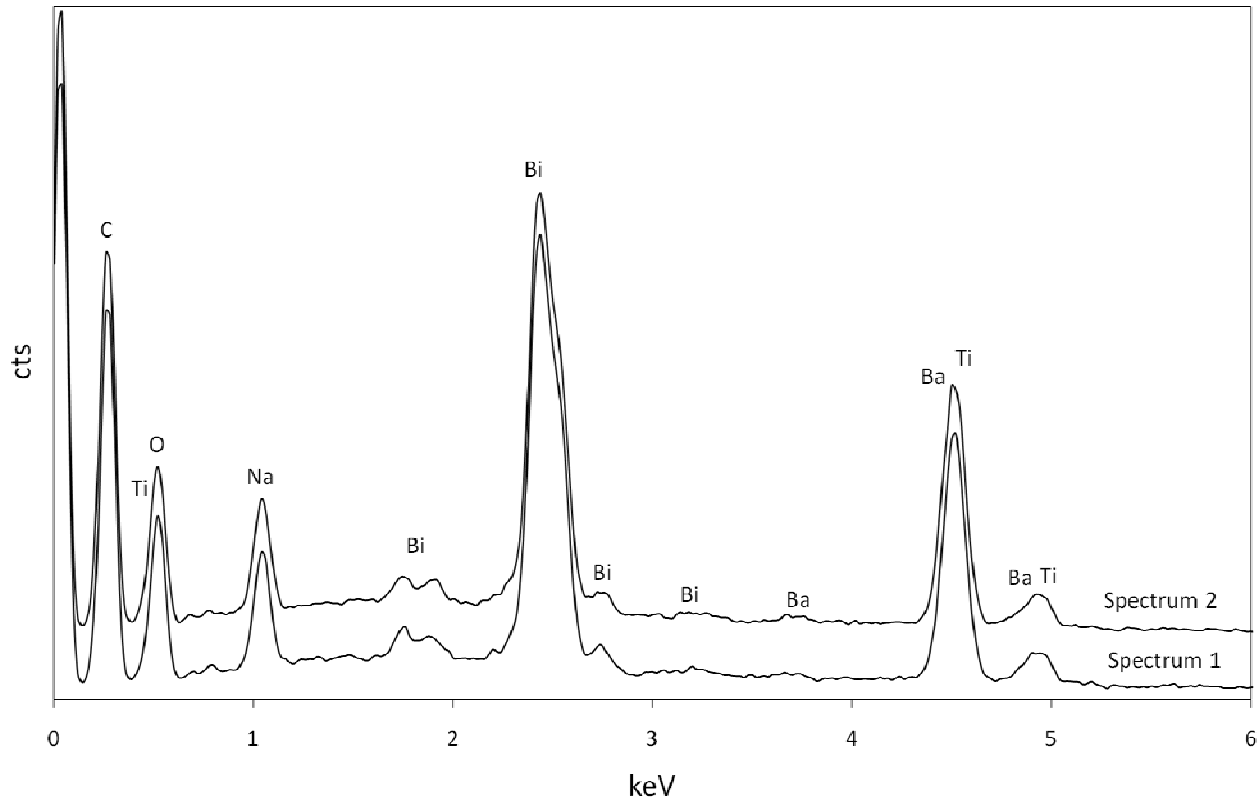

Figure 3(b). “Piezoelectric properties of lead-free Submicron-structured …”L. Pardo et al.

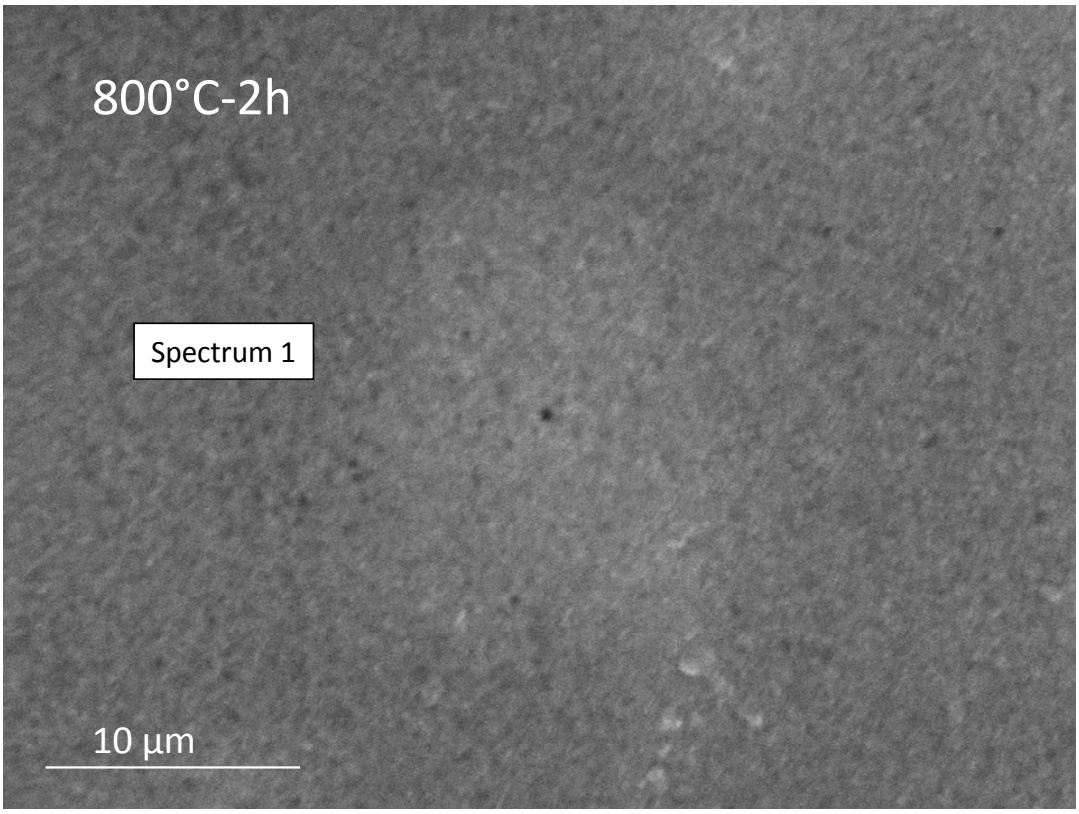

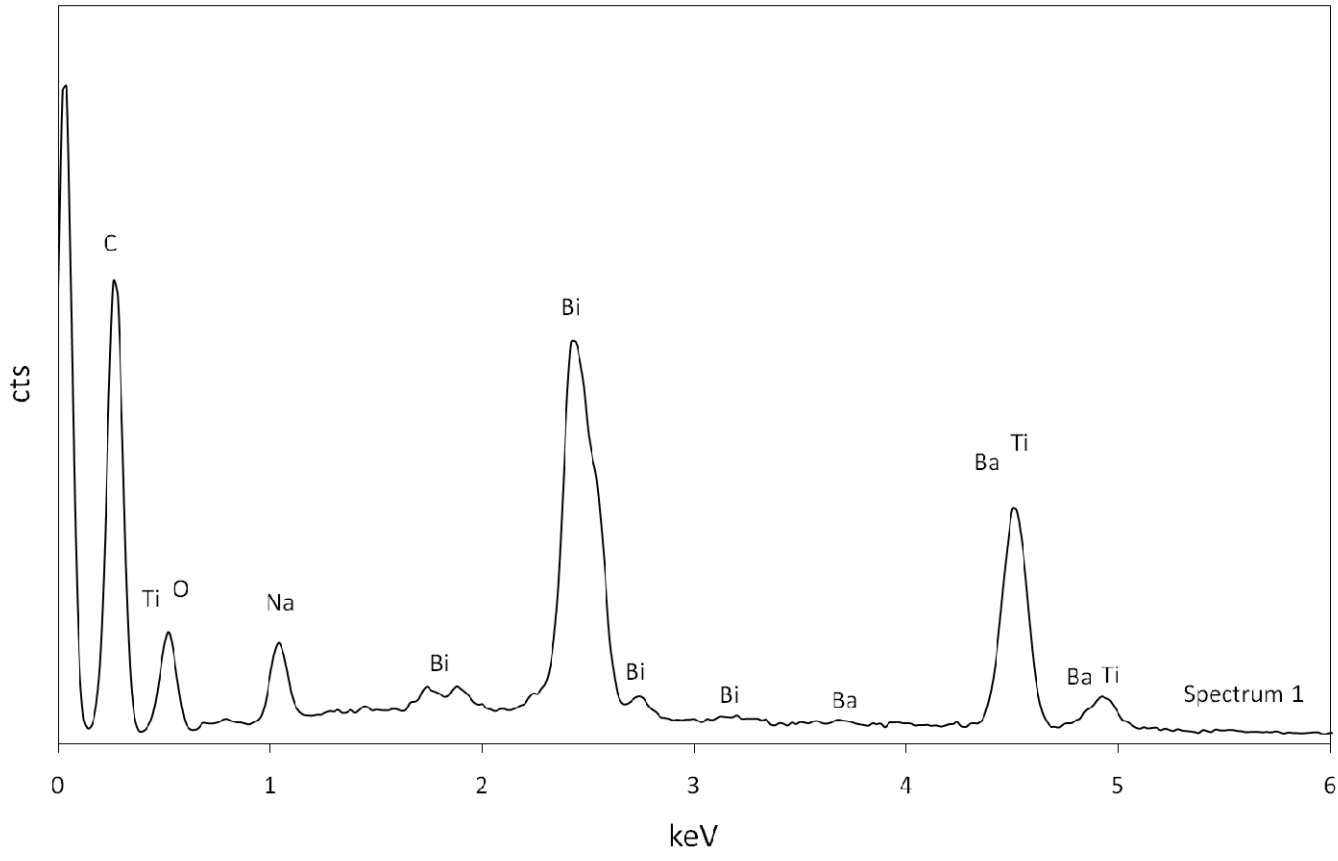

Figure 3(c). “Piezoelectric properties of lead-free Submicron-structured …”L. Pardo et al.

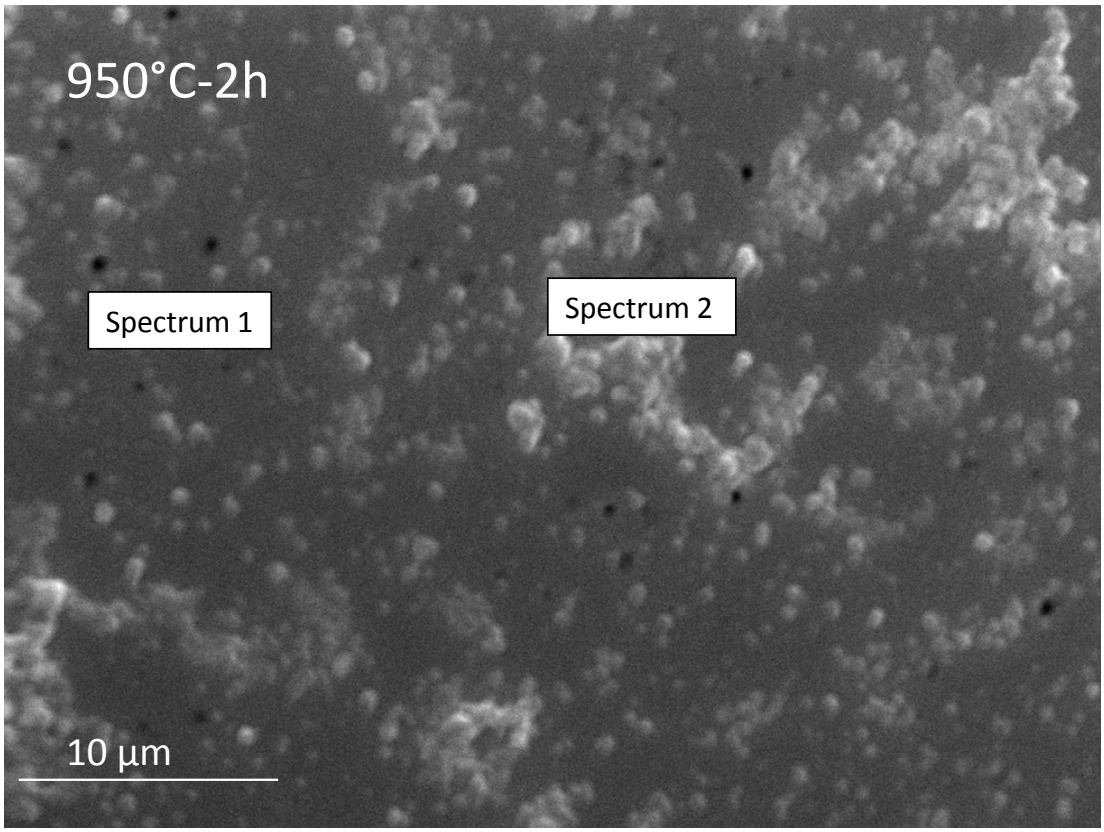
950°C-2h
Spectrum 1
Spectrum 2
10 µm

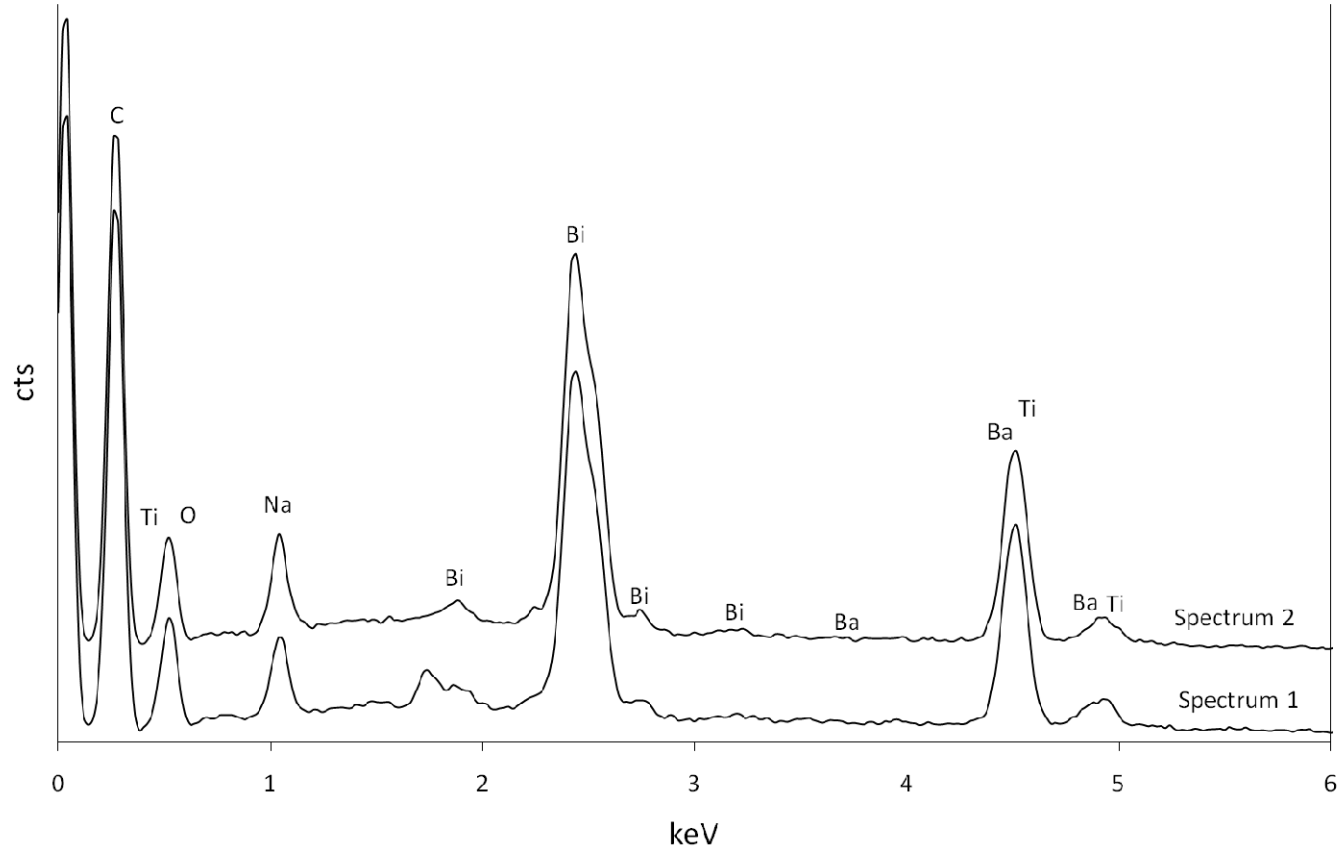
cts
C
Ti
O
Na
Bi
Bi
Bi
Bi
Ba
Ba
Ti
Ba Ti
Spectrum 2
Spectrum 1
0
1
2
3
4
5
6
keV

Figure 4.

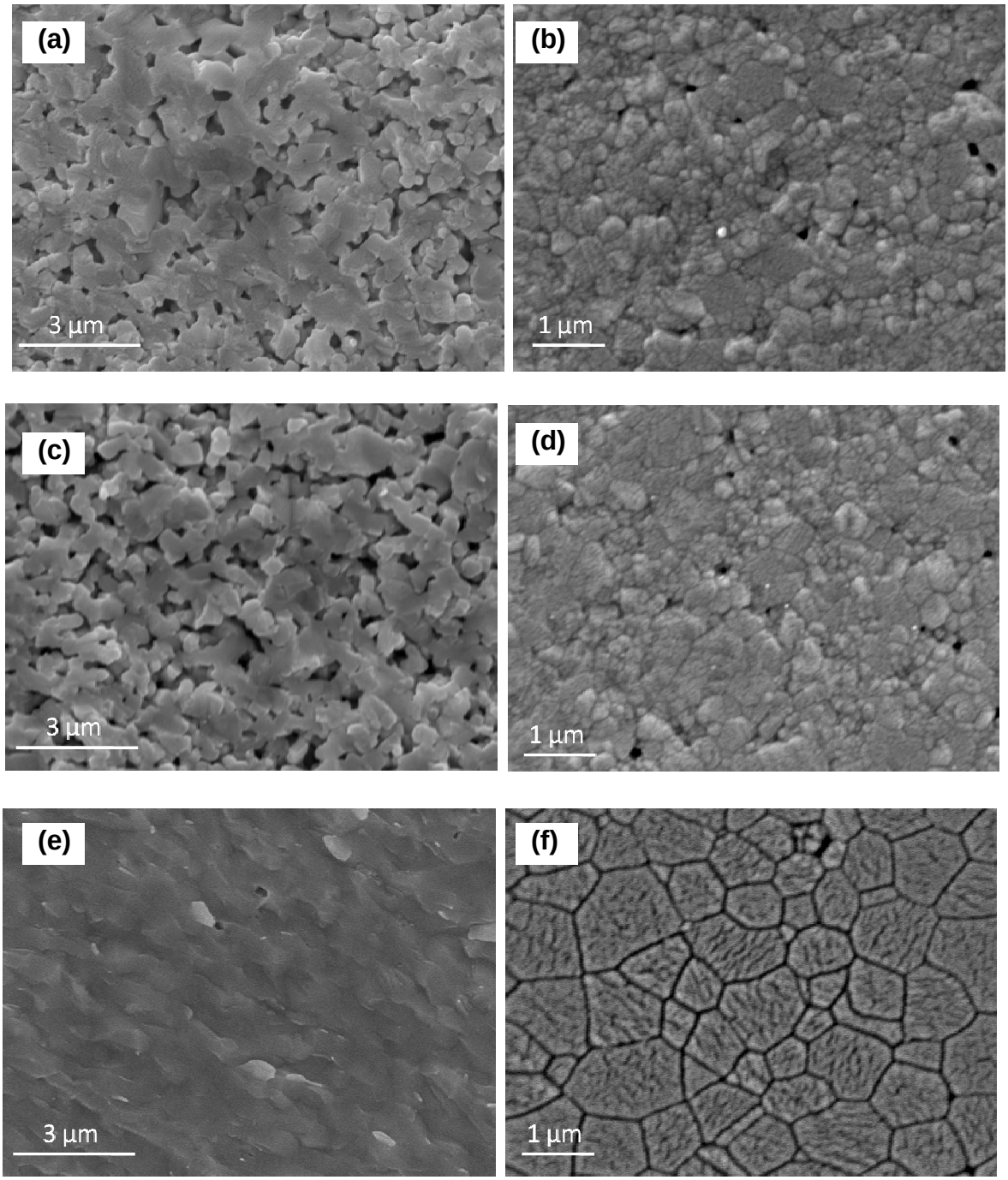

“Piezoelectric properties of lead-free Submicron-structured …”
L. Pardo et al.

Figure 5.

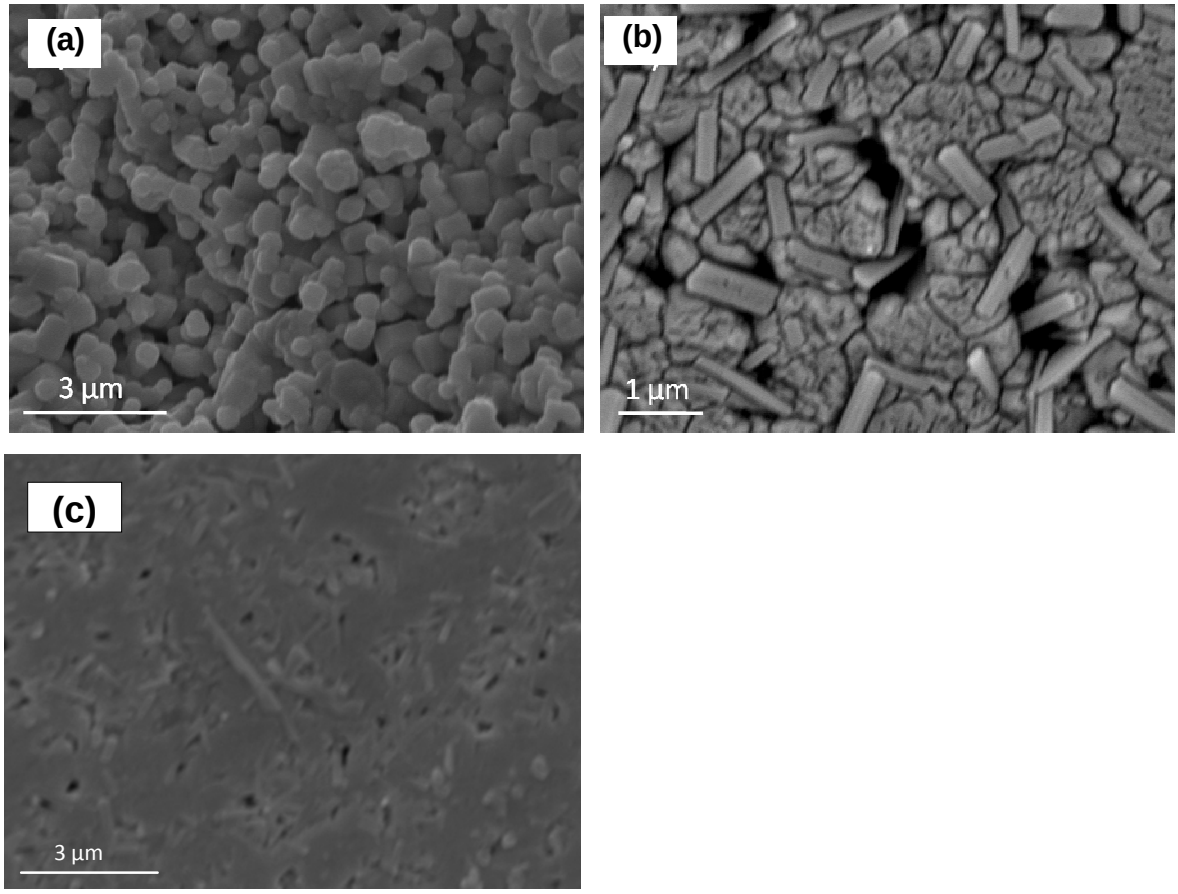

“Piezoelectric properties of lead-free Submicron-structured …”
L. Pardo et al.

Figure 6.

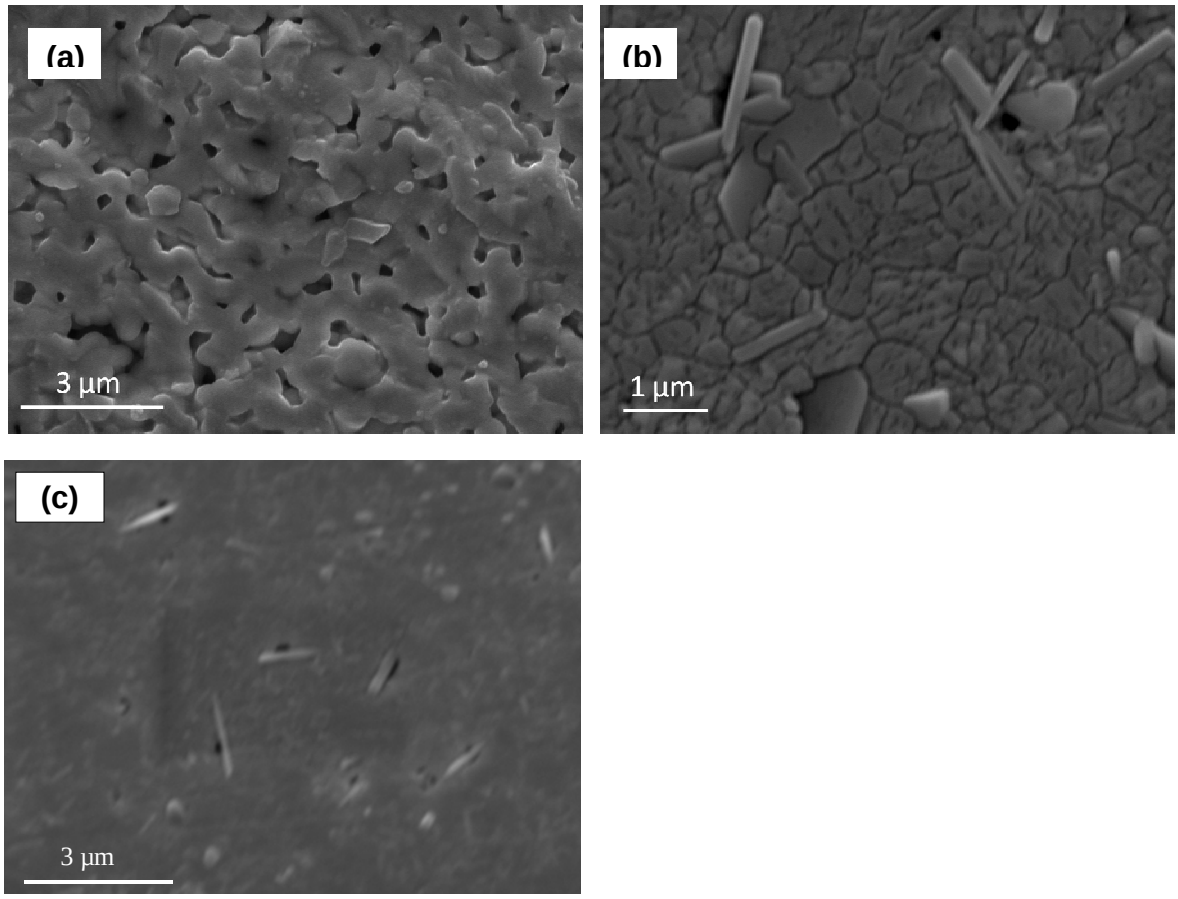

“Piezoelectric properties of lead-free Submicron-structured …”
L. Pardo et al.

Figure 7.

"Piezoelectric properties of lead-free Submicron-structured …"
L. Pardo et al.

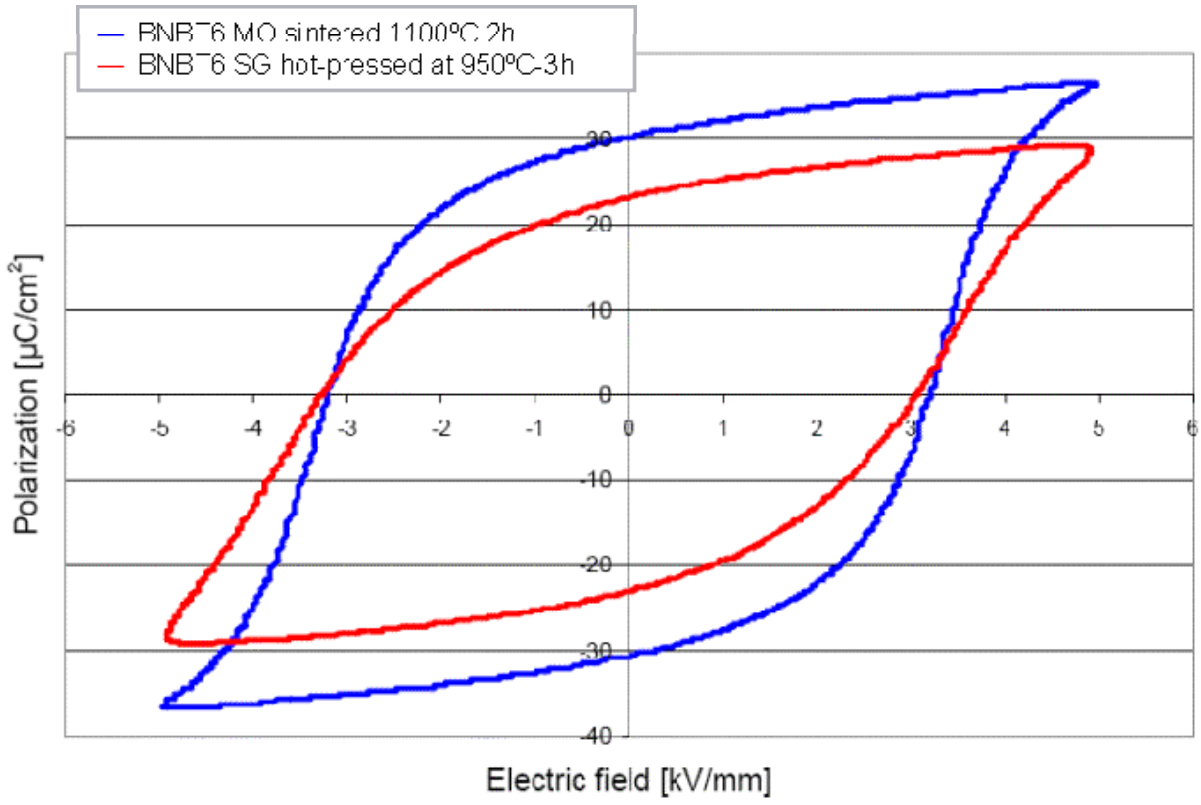

Figure 8.

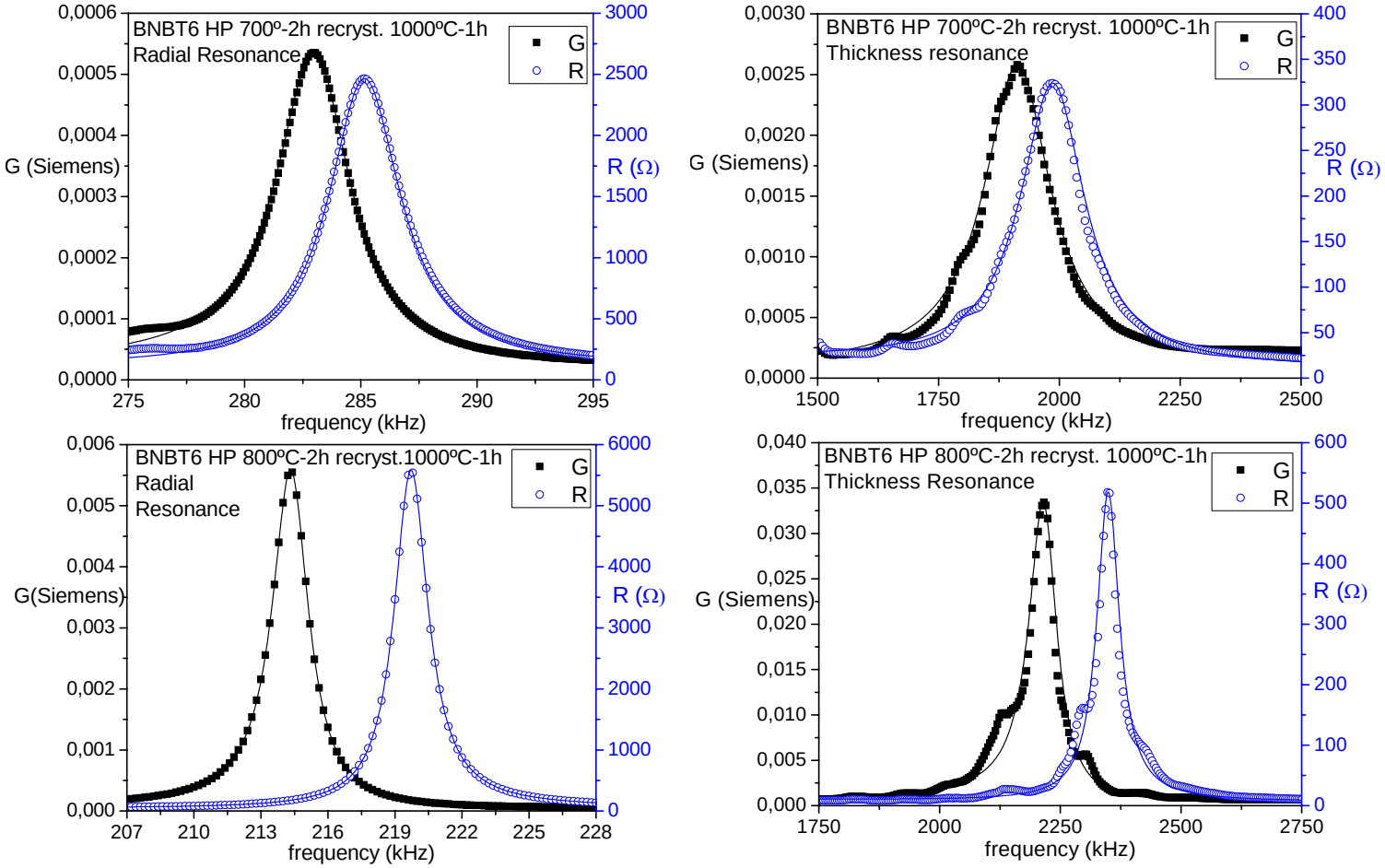
BNBT6 HP 700º-2h recryst. 1000ºC-1h
Radial Resonance
G
R
G (Siemens)
R (Ω)
frequency (kHz)
BNBT6 HP 700ºC-2h recryst. 1000ºC-1h
Thickness resonance
G
R
G (Siemens)
R (Ω)
frequency (kHz)
BNBT6 HP 800ºC-2h recryst.1000ºC-1h
Radial
Resonance
G
R
G(Siemens)
R (Ω)
frequency (kHz)
BNBT6 HP 800ºC-2h recryst. 1000ºC-1h
Thickness Resonance
G
R
G (Siemens)
R (Ω)
frequency (kHz)